Membrane Assembly of M13 Major Coat Protein: Evidence for a Structural Adaptation in the Hinge Region and a Tilted Transmembrane Domain

Ruud B. Spruijt,* Cor J. A. M. Wolfs, and Marcus A. Hemminga

Laboratory of Biophysics, Wageningen University, Dreijenlaan 3, 6703 HA Wageningen, The Netherlands

Received July 22, 2004; Revised Manuscript Received August 30, 2004

ABSTRACT: New insights into the low-resolution structure of the hinge region and the transmembrane domain of the membrane-bound major coat protein of the bacteriophage M13 are deduced from a single cysteine-scanning approach using fluorescence spectroscopy. New mutant coat proteins are labeled and reconstituted into phospholipid bilayers with varying headgroup compositions (PC, PE, and PG) and thicknesses (14:1PC, 18:1PC, and 22:1PC). Information about the polarity of the local environment around the labeled sites is deduced from the wavelength of maximum emission using AEDANS attached to the SH groups of the cysteines as a fluorescent probe. It is found that the protein is almost entirely embedded in the membrane, whereas the phospholipid headgroup composition of the membrane hardly affects the overall embedment of the protein in the membrane. From the assessment of a hydrophobic and hydrophilic face of the transmembrane helix, it is concluded that the helix is tilted with respect to the membrane normal. As compared to the thicker 18:1PC and 22:1PC membranes, reconstitution of the protein in the thin 14:1PC membranes results in a loss of helical structure and in the formation of a stretched conformation of the hinge region. It is suggested that the hinge region acts as a flexible spring between the N-terminal amphipathic arm and transmembrane hydrophobic helix. On average, the membrane-bound state of the coat protein can be seen as a gently curved and tilted, "banana-shaped" molecule, which is strongly anchored in the membrane−water interface at the C-terminus. From our experiments, we propose a rather small conformational adaptation of the major coat protein as the most likely reversible mechanism for responding to environmental changes during the bacteriophage disassembly and assembly process.

Upon infection of *Escherichia coli*, the filamentous bacteriophage M13 disassembles with the major coat protein (see Figure 1A) becoming stably inserted in the bacterial inner membrane (*1*, *2*). The membrane-bound protein is an excellent system for studying fundamental aspects of protein−lipid interactions. These interactions are important for the correct membrane assembly of this protein, but also for membrane proteins in general (*3*).

The M13 major coat protein possesses interesting physicochemical characteristics affecting the protein−lipid interactions. The protein can roughly be divided into three structural domains (Figure 1B). NMR studies of the protein in SDS[1] micelles and in oriented membranes revealed the presence of a stable hydrophobic α-helix and a less stable N-terminal amphipathic α-helix (*4*−*6*). A distorted helical hinge region connects both helices. In detergent micelles, these three structured segments of the protein are well-defined, but not with respect to each other, due to flexibility in the hinge region. In phospholipid bilayers, however, an angle of approximately 90° between the amphipathic N-terminal helix and the transmembrane hydrophobic helix has been reported (*6*−*9*). Recently, a gradual membrane-entering N-terminal arm and the presence of a tilted hydrophobic helix have been proposed, suggesting a less pronounced configuration (*10*−*12*). In this view, it should be noted that, when the coat protein is part of the M13 phage particle, it is arranged in one continuous, slightly bent helix (Figure 1E) (*13*). No information about factors directing the rearrangement of the two helices from the membrane-bound to the viral-bound state of the protein during the membrane-bound phage assembly process is available.

Much is known about the aggregational behavior and overall conformation of the M13 major coat protein when it is embedded in phospholipid bilayers (*14*−*17*). Marvin (*1*) critically reviewed the numerous aspects related to this subject. Usually, X-ray crystallography and high-resolution NMR spectroscopy are applied to gain structural information about proteins. However, these techniques are often restricted to elucidating the conformational state of water-soluble proteins (*18*). Recently, a solid-state NMR approach was successfully applied to determine the structure of the membrane-bound form of the Fd coat protein in oriented lipid

* To whom correspondence should be addressed. Telephone: +31-317-482044. Fax: +31-317-482725. E-mail: ruud.spruijt@wur.nl.

[1] Abbreviations: 14:1PC, dimyristoleoylphosphatidylcholine; 16:1PC, dipalmitoleoylphosphatidylcholine; 18:1PC, dioleoylphosphatidylcholine; 20:1PC, dieicosenoylphosphatidylcholine; 22:1PC, dierucoylphosphatidylcholine; DOPC, dioleoylphosphatidylcholine; DOPE, dioleoylphosphatidylethanolamine; DOPG, dioleoylphosphatidylglycerol; HPSEC, high-performance size exclusion chromatography; IAEDANS, *N*-(iodoacetylaminoethyl)-5-naphthylamine-1-sulfonic acid; L/P, lipid-to-protein molar ratio; λ_{max}, wavelength of maximum emission; PAGE, polyacrylamide gel electrophoresis; SDS, sodium dodecyl sulfate; TFE, trifluoroethanol; MeOH, methanol; DMSO, dimethyl sulfoxide; DMF, dimethylformamide; K_{sv}, Stern−Volmer constant; CD, circular dichroism.

10.1021/bi048437x CCC: $27.50
Published on Web 10/16/2004

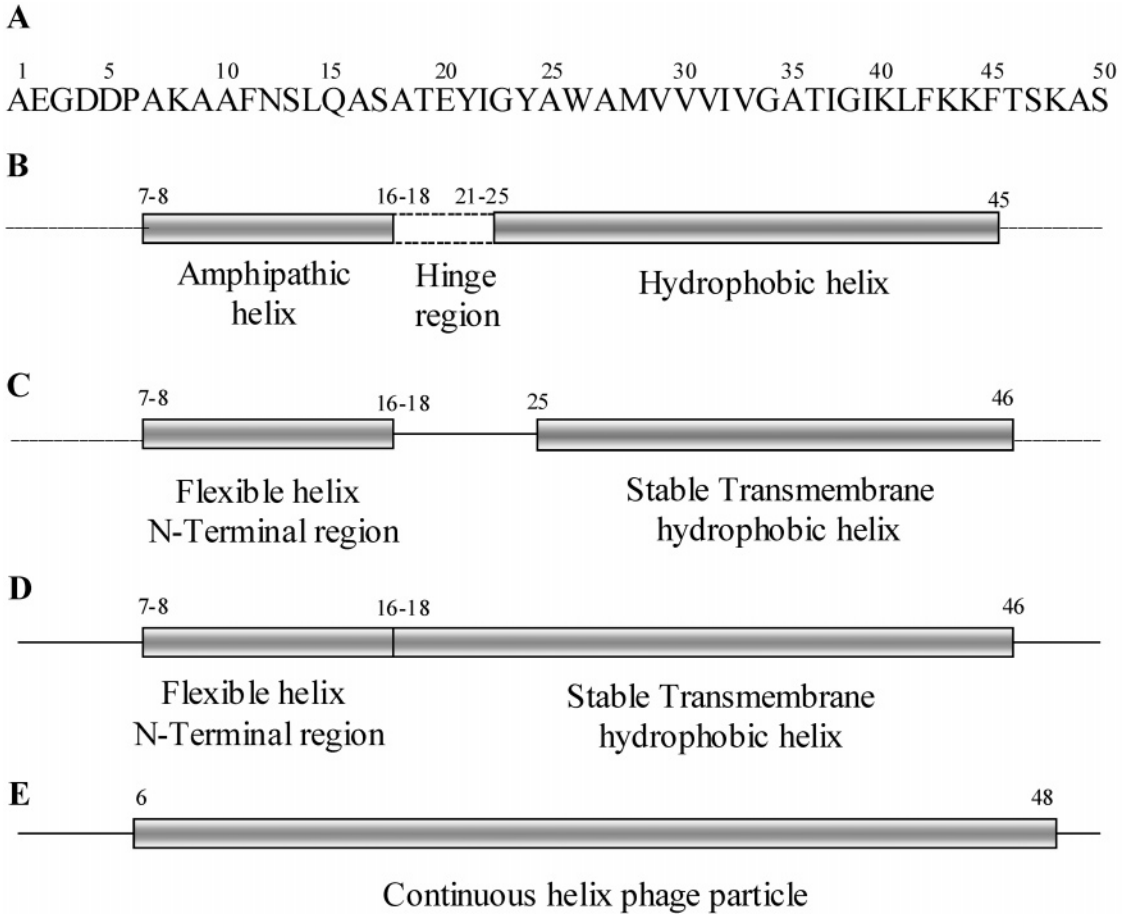

FIGURE 1: (A) Primary structure of the M13 major coat protein (the product of M13 gene VIII). (B) Secondary structure as determined from NMR studies of the protein in SDS micelles and membranes (*4*−*6*). (C and D) Assignment of the secondary structure of the protein in lipid bilayers as determined in this study. The situation depicted in panel D refers to the protein reconstituted into 18:1PC (and to a less extent 22:1PC) membranes. In the case that the protein is reconstituted into 14:1PC membranes, the helical conformation in the hinge region is partly lost (on average) and results in a more stretched conformation (C). In this view, the hinge region acts as a flexible spring between the N-terminal amphipathic helix and the transmembrane hydrophobic helix. (E) Secondary structure of the major coat protein when part of the bacteriophage M13 particle (*13*).

bilayers (*6*). Here we offer an alternative technique for obtaining additional structural information about membrane proteins in phospholipid membranes. Many new insights about the membrane-bound state of the M13 major coat protein originate from the site-directed introduction of reporter groups, such as fluorescent labels or spin-labels (*10*, *17*, *19*−*21*).

In this paper, a series of new coat protein mutants containing a single cysteine residue in the hinge region and transmembrane domain is presented. The local polarity of a fluorescent probe attached to the introduced single cysteine residue of the protein is acquired and is related to its membrane penetration. The fluorescent environmental probe *N*-(iodoacetylaminoethyl)-5-naphthylamine-1-sulfonic acid (AEDANS) is used. The fluorescence properties and accessibilities toward various quencher molecules are reported to be dependent on polarity as well as steric effects (*10*, *22*). The membrane-bound state of the labeled protein is examined in phospholipid bilayers with different headgroup compositions and hydrophobic thicknesses. Determination of the relative depth of specific sites of the coat protein reveals aspects about membrane anchoring, formation of local structure in the hinge region, and the observation of a tilted state of the transmembrane helix of the M13 major coat protein.

EXPERIMENTAL PROCEDURES

Materials. Dimyristoleoylphosphatidylcholine (14:1PC), dipalmitoleoylphosphatidylcholine (16:1PC), dioleoylphosphatidylcholine (DOPC, 18:1PC), dieicosenoylphosphatidylcholine (20:1PC), dierucoylphosphatidylcholine (22:1PC), dioleoylphosphatidylglycerol (DOPG), and dioleoylphosphatidylethanolamine (DOPE) were purchased from Avanti Polar Lipids. IAEDANS was obtained from Molecular Probes. Sodium cholate was acquired from Sigma-Aldrich. All other chemicals of pro-analytical grade were obtained from Merck unless stated otherwise.

Preparation and Purification of Labeled Cysteine-Containing Major Coat Protein Mutants. The cloning and site-directed mutagenesis procedure is described in detail elsewhere (*10*). M13 major coat protein mutants were isolated using reversed phase chromatography, labeled with AEDANS, and further purified as previously described in detail (*10*). An additional polishing step was part of the purification protocol and included HPSEC on a Superdex 75 pg HR 16/50 column (Amersham Biosciences) eluted with 50 mM sodium cholate in 10 mM Tris-HCl (pH 8.0), 0.2 mM EDTA, and 150 mM NaCl. The labeled coat protein stock solutions were checked for purity, protein content, and absence of specific or irreversible protein aggregates using Tricine

SDS−PAGE (*23*) and subsequent immunodetection. Mutant major coat proteins with a cysteine at position 36, 38, or 49 were obtained, labeled with IAEDANS, and purified as described previously (*19*).

Reconstitution of the AEDANS-Labeled Coat Protein into Phospholipid Bilayers. Unless stated otherwise, the labeled coat protein mutants were reconstituted into phospholipids using the cholate dialysis procedure under saline conditions as described previously (*14*, *24*). The concentration of labeled coat protein was kept constant at 5 μM. The final molar lipid-to-protein ratio was ~250. The resulting proteoliposomes in 10 mM Tris-HCl (pH 8.0), 0.2 mM EDTA, and 150 mM NaCl were used for fluorescence measurements after a short low-speed centrifugation to remove irregularities.

Steady-State Fluorescence Measurements. The fluorescence properties of the AEDANS-labeled major coat protein were recorded at room temperature on a Perkin-Elmer LS-5 luminescence spectrophotometer. The excitation wavelength was 340 nm, and emission scans were routinely recorded from 460 to 530 nm, unless stated otherwise. Excitation and emission slits were set at 5 nm. Samples (1 mL) were in Hellma model 114F-QS cuvettes (10 mm × 4 mm light paths). The optical density at the excitation wavelength (1 cm light path) never exceeded 0.1. Fluorescence intensities were corrected for background by subtracting the spectrum of the unlabeled wild-type major coat protein, reconstituted into the same phospholipid bilayers, and recorded under the same conditions. As has been mentioned in a previous paper (*10*), the wavelength of maximum emission intensity showed a 8 nm red shift as compared to the results reported in ref *19*. This was due to a different instrumental setup of the luminescence spectrophotometer. The wavelength of maximum emission was routinely taken from a smoothed, wide-plotted top part of the background-corrected emission spectrum. The error of the measured wavelengths of maximum emission (λ_{max}) is found to be within 1 nm.

Steady-state quenching studies were performed by adding various amounts of an acrylamide stock solution [2.67 M acrylamide in 10 mM Tris-HCl (pH 8.0), 0.2 mM EDTA, and 150 mM NaCl] to a final concentration of 0.348 M. Emission spectra were recorded at least 1 min after each addition of the acrylamide stock solution, and the stable fluorescence intensities were corrected for background effects and dilution. The error of the calculated Stern−Volmer quenching constant (K_{sv}) values is ±5%.

Circular Dichroism Measurements. Circular dichroism spectra were recorded from 200 to 250 nm on a JASCO 715 spectrometer equipped with a Peltier device PTC-348 WI at room temperature using a cell with a path length of 1 mm. The CD settings were as follows: scan time of 100 s, bandwidth of 1 nm, resolution of 0.1 nm, and response time of 125 ms. Up to 50 spectra were accumulated to improve the signal-to-noise ratio. Background spectra were recorded under the same experimental conditions and were subtracted from the corresponding spectra. For the purpose of CD, the major coat protein was reconstituted into phospholipid bilayers of 14:1PC to 22:1PC using the cholate dialysis reconstitution procedure in 100 mM NaP_i buffer (pH 8.0).

RESULTS

Expression and Aggregation Characterization of Mutant M13 Major Coat Protein. In addition of the previously described single cysteine mutants (*10*, *19*), a series of new coat protein mutants was produced containing a single cysteine residue at position 16, 18, 20, 25, 27−35, 37, 39, 41−44, 46, 47, or 50. All overexpressed coat protein mutants are successfully inserted into the *E. coli* cytoplasmic membrane, as observed by the correct processing by the *E. coli* leader peptidase (data not shown). The majority of overexpressed single-cysteine mutants migrated on gel in a manner identical, and with similar intensities, to that of the wild-type protein, without the presence of any β-sheet polymers (*24*). Although the unlabeled mutants with a cysteine residue at positions 21, 22, 27, 39, 42, and 46 are found to be partly in a monomer−dimer equilibrium state on the SDS gel, they are mainly monomeric after labeling (data not shown). An exception is mutant V30C, which appeared to be almost completely dimeric on the SDS gel, irrespective of labeling.

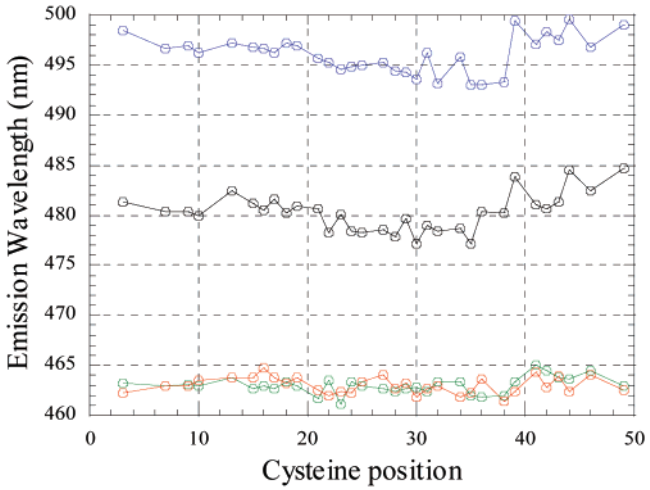

FIGURE 2: Wavelength of maximum emission (λ_{max}) of AEDANS attached to different positions along the primary structure of the M13 major coat protein mutants solubilized in 90% (v/v) TFE (protic solvent, blue circles), in 90% (v/v) MeOH (protic solvent, black circles), in 90% (v/v) DMSO (aprotic solvent, green circles), and in 90% (v/v) DMF (aprotic solvent, red circles). The coat protein concentration was 5 μM.

Environmental Polarity Probing in a Homogeneous Protein Surrounding. To rule out the possibility that variation in the wavelength of maximum emission (λ_{max}) is caused by differences in the local polarity within the coat protein itself, the protein was brought into a homogeneous environment. For these experiments, we applied two protic organic solvents (TFE and MeOH) and two aprotic organic solvents (DMSO and DMF) at a concentration of 90% (v/v) in buffer. The λ_{max} values of the coat protein mutants in these solvents are given in Figure 2. Apart from the (very) different wavelength levels, the local effects of the protein backbone and neighboring amino acid residues within one series are small, especially in the case of aprotic solvents DMSO and DMF. The calculated mean λ_{max} values per solvent series were subtracted from the original data. The resulting differences in the λ_{max} values per labeled position were then averaged for all four solvent series, supplemented with a value of 465 nm, and plotted in the bottom part of Figure 4. As can be seen in Figure 4, these averaged differences of λ_{max} values, due to local polarity effects within the protein, are slightly negative for those positions that constitute the hydrophobic TM domain of the coat protein. Around the basic C-terminal

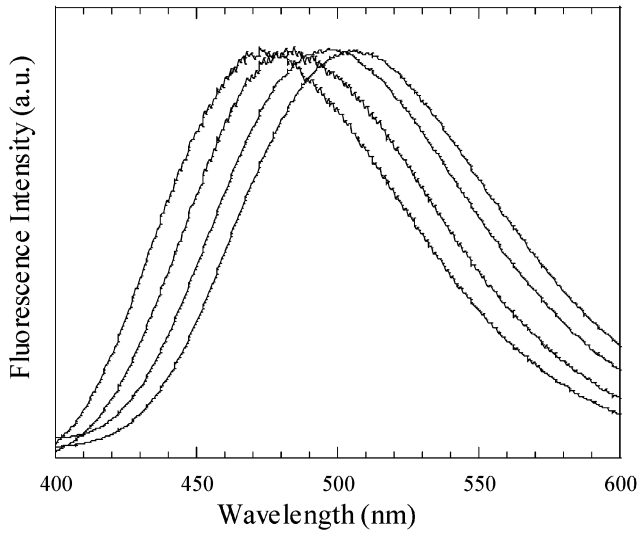

FIGURE 3: Normalized fluorescence emission spectra of AEDANS-labeled M13 major coat protein mutants reconstituted into 80% DOPC/20% DOPG (molar ratio) membranes at L/P = 250. The AEDANS label is attached to positions (curves from left to right) 34, 25, 13, and 3 of the primary sequence of the protein.

end of the protein, the averaged differences in λ_{max} values are somewhat positive.

Both the initial λ_{max} values of the AEDANS-labeled major coat protein in DOPC/DOPG membranes (empty symbols) and the λ_{max} profile after correction for local polarity effects within the protein (solid symbols and line) are presented in Figure 4. As can be seen, the influence of backbone or neighboring amino acid residues is quite small. Nevertheless, all λ_{max} values presented in Figures 5−7 are corrected for this effect. Therefore, the local polarity caused by the protein itself can be neglected in the following experiments, where the protein environment is imposed by a phospholipid bilayer.

Environmental Probing Using AEDANS-Labeled Protein in DOPC/DOPG Membranes. Figure 3 shows typical fluorescence spectra of some AEDANS-labeled M13 major coat protein mutants reconstituted into DOPC/DOPG membranes. The spectra are clearly shifted to longer wavelengths going from labeling position 34 toward position 3. The overall line shapes appeared to be identical for all mutants. On average, the peak widths ranged between 100 and 105 nm. Therefore, it is assumed that the conformation and dynamics of the probe are invariant. The AEDANS label at position 34 is assumed to penetrate the membrane, whereas the label attached to the protein at amino acid residue 3 is in a polar environment at the outside of the membrane (*10*, *19*).

In Figure 4, the λ_{max} values for AEDANS-labeled major coat protein mutants reconstituted into DOPC/DOPG membranes are plotted together with a six-term polynomial curve fit. On top of this mainly V-shaped trend line, a fine structure of λ_{max} values is observed with relative high values at amino acid residue positions 9, 13, 16, 17, 20, 23, 24, 27, 28, 30, 31, 36, 39, and 43. In contrast, relatively low λ_{max} values are found at positions 15, 18, 19, 22, 25, 29, 33−35, 37, 38, and 46.

Environmental Probing Using AEDANS Fluorescence in Membranes with Varying Phospholipid Headgroup Compositions. Figure 5 shows the wavelength of maximum emission (λ_{max}) of AEDANS, attached to different positions of the M13 major coat protein mutants reconstituted in membranes with

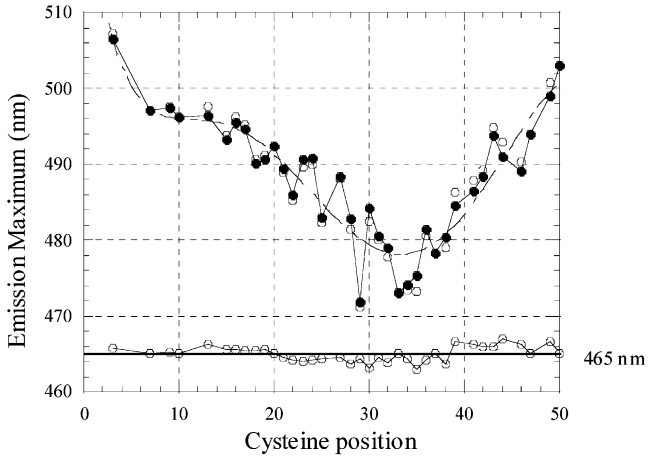

FIGURE 4: Wavelength of maximum emission (λ_{max}) of AEDANS attached to different positions along the primary structure of the M13 major coat protein mutants reconstituted into 80% DOPC/20% DOPG (molar ratio) membranes at L/P = 250. λ_{max} values of AEDANS-labeled protein mutants are shown before (○) and after (●) correction for the differences in the local polarity caused by the coat protein itself (○ at the bottom of the plot). A six-term polynomial curve fit of the corrected λ_{max} profile (●) is depicted in the plot as a dashed line. The averaged differences in local polarity effects, calculated from the experimental λ_{max} profiles (Figure 2), and supplemented with 465 nm, are presented at the bottom of the plot. The coat protein concentration was 5 μM.

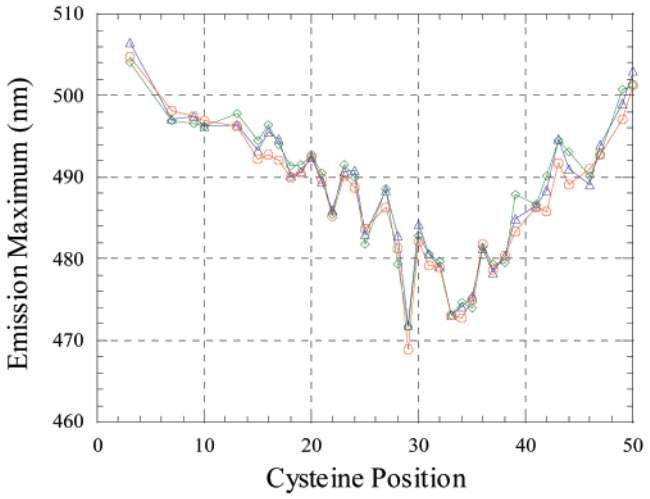

FIGURE 5: Wavelength of maximum emission (λ_{max}) of AEDANS attached to different positions along the primary structure of the M13 major coat protein mutants reconstituted into membranes with a different phospholipid headgroup composition. λ_{max} values of AEDANS-labeled protein mutants reconstituted into 80% DOPC/20% DOPG (molar ratio) membranes at L/P = 250 (blue triangles), in pure DOPC at L/P = 250 (red circles), and in 70% DOPE/30% DOPG (molar ratio) membranes at L/P = 100 (green diamonds). Some data points of the DOPC/DOPG line were included from a previous study (*10*). The coat protein concentration was 5 μM.

a different phospholipid headgroup composition. For this purpose, the series of newly prepared labeled mutants (described above) were supplemented with a number of mutants from previous studies (*10*, *19*). As can be observed, the λ_{max} values of the AEDANS-labeled major coat protein mutants reconstituted into pure DOPC and DOPC/DOPG and DOPE/DOPG mixtures are quite similar. Most of the minor variations in λ_{max} values between these phospholipid mixtures are observed at positions close to the phospholipid headgroup region. In these cases, the λ_{max} values found in DOPC/DOPG

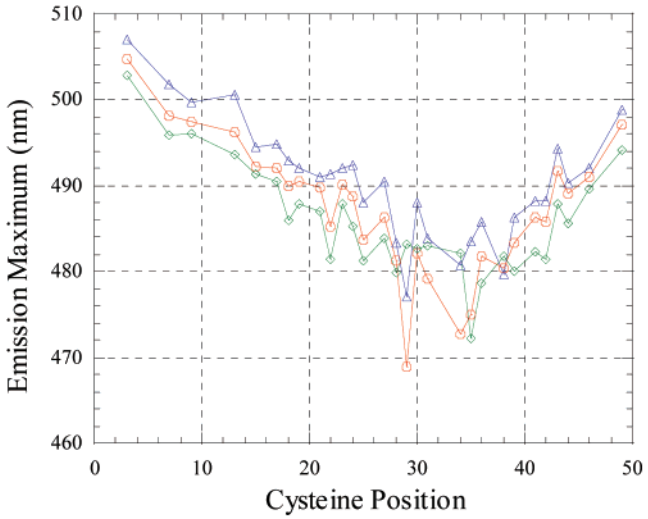

FIGURE 6: Wavelength of maximum emission (λ_{max}) of AEDANS attached to different positions along the primary structure of the M13 major coat protein mutants reconstituted into diacylphosphatidylcholine (PC) membranes with a varying bilayer thickness at L/P = 250: 14:1PC (blue triangles), 18:1PC (red circles), and 22:1PC (green diamonds). The coat protein concentration was 5 μM.

and DOPE/DOPG membranes are slightly higher as compared to those obtained for pure DOPC.

Environmental Probing in Response to Variation of Membrane Thickness. Figure 6 shows the λ_{max} values of AEDANS-labeled major coat protein mutants reconstituted into diacylphosphatidylcholine (PC) membranes with a varying bilayer thickness. For this purpose, we used PC-containing monounsaturated acyl chains: 14:1PC, 18:1PC (DOPC), and 22:1PC. The hydrophobic thicknesses of these bilayers, defined as the distance between the carbonyl moieties of two opposing lipids, are 22.5, 29.5, and 36.5 Å, respectively (*25*, *26*).

For most of the labeled mutants, the λ_{max} values decrease when the membrane thickness is increased and the λ_{max} plots are roughly parallel. An exception is, however, found at positions 28−38 in the thickest membrane (22:1PC), showing λ_{max} values around 480 nm, whereas lower values could be expected (see the tendencies for the λ_{max} values of the other label positions in Figure 6). The peak widths found for positions 28−38 in the 22:1PC membrane ranged between 100 and 105 nm, which is identical to the range observed for the other labeled positions or other membrane compositions.

A closer look at the plots in Figure 6 reveals some more differences, especially in the hinge region of the protein. This is exemplified in Figure 7A which shows the range from amino acid residue 17 to 25. When the bilayer thickness is increased from 14:1PC to 22:1PC, the λ_{max} values, especially at positions 18 and 22, significantly decrease as compared to the λ_{max} values of the other positions.

Since it is known that the accessibility of the AEDANS fluorophore to a quencher molecule depends on the polarity and steric effects (*10*, *27*), the quenching efficiency can provide additional information about the local surrounding of this hinge region of the protein. For these quenching experiments, the polar but uncharged acrylamide quencher molecule acrylamide is used. The acrylamide quenching results are shown in Figure 7B. When the bilayer thickness is increased from 14:1PC to 22:1PC, the quenching constants

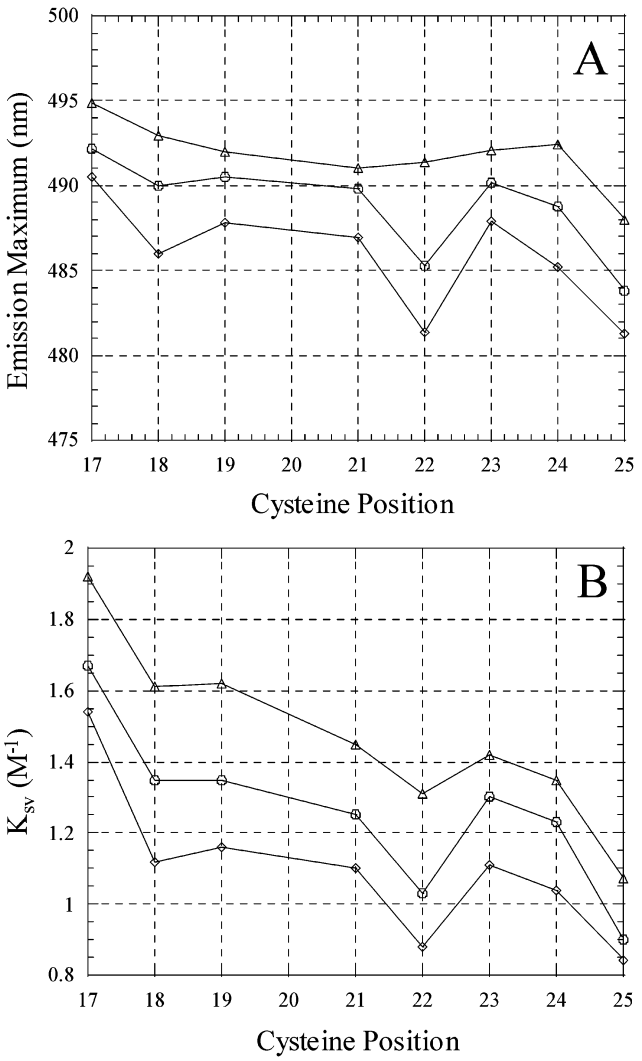

FIGURE 7: Detailed plot of the λ_{max} values (A) and acrylamide quenching profile (B) of AEDANS attached to positions 17−25 of the M13 major coat protein mutants reconstituted into diacylphosphatidylcholine (PC) membranes with a varying bilayer thickness at L/P = 250: 14:1PC (△), 18:1PC (○), and 22:1PC (◇). The coat protein concentration was 5 μM.

(as calculated from a series of concentration-dependent experiments) are lower. With an increasing bilayer thickness, the quenching efficiencies at positions 18 and especially 22 are significantly decreased compared to those of their neighboring positions.

The overall conformation of the M13 major coat protein reconstituted into diacylphosphatidylcholine (PC) membranes with a varying bilayer thickness was determined using circular dichroism spectroscopy. The ratios of ellipticities monitored at 210 and 222 nm, which is a measure of helical content, as a function of different acyl chain length are given in Figure 8. From the 14:1PC to the 22:1PC system, there is initially an increase in the ratio up to the 18:1PC system, after which the ratio strongly decreases. The highest value of the ratio is ~0.96, which is indicative of an almost 100% helical conformation (*28*).

DISCUSSION

AEDANS-Labeled M13 Major Coat Protein Mutant Approach. With the fluorescence probe AEDANS attached to the cysteine residues of the M13 major coat protein mutants,

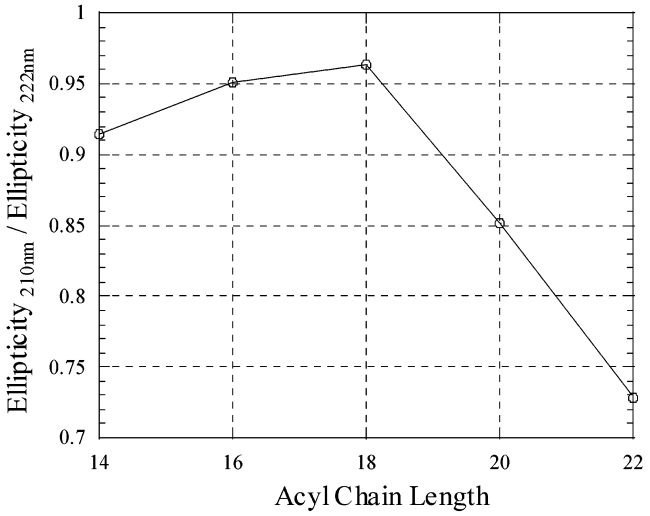

FIGURE 8: Ratios of CD intensities at 210 and 222 nm of the M13 major coat protein reconstituted into diacylphosphatidylcholine (PC) membranes with acyl chain lengths varying from 14:1PC to 22:1PC.

we monitored the polarity of the local environment at defined positions of the protein in the membrane. This property of AEDANS provides information about the extent of membrane penetration of the labeled site. The λ_{max} of AEDANS varies from 520 nm in an aqueous environment to 448 nm in pure dimethylformamide (*22*). Previously, it was shown that λ_{max} is highly sensitive to changes in penetration depth in the membrane, when attached to single-cysteine mutants of the M13 major coat protein (*10*, *11*, *19*). Further information obtained from the accessibility of fluorescence quencher molecules acrylamide (see also Figure 7) and 5-doxylstearic acid supports these changes in penetration depth in the membrane (*10*).

The application of a series of new single-cysteine mutants, in addition to those previously reported, significantly contributed to better insight into the membrane-bound state of the coat protein. Therefore, the cysteine-scanning approach appears to be very useful, especially when as many protein mutants as possible are available. At this moment, 40 of a total of 50 amino acids of the major coat protein have been substituted for AEDANS-labeled single-cysteine residues. All overexpressed coat protein mutants are checked for the correct insertion into the *E. coli* cytoplasmic membrane and subsequent processing by the *E. coli* leader peptidase. This justifies a study of the membrane-bound state of these M13 major coat protein mutants. By application of phospholipids containing unsaturated acyl chains and high L/P ratios under saline conditions, exclusive information about the lipid environment of the labeled major coat protein could be obtained (*14*). The local effects of the protein backbone or neighboring amino acid residues are small (see Figures 2 and 4). A recent quantitative fluorescence analysis using the Stokes shift of AEDANS-labeled cysteine mutants of the M13 major coat protein incorporated in lipid bilayers offers a reliable description of the lipid bilayer topology of the protein and bilayer properties (*29*). This also indicates that the spacer link between the protein and AEDANS label is long enough for monitoring the local polarity of the lipid environment and not that of the amino acid residues of the protein, and short enough that the topology of the protein imposes on the fluorescence properties of the AEDANS label. This clearly indicates that the observed differences in the emission maximum of the AEDANS probe can be related to differences in the position and orientation of the labeled cysteine position in the native protein (*29*). Therefore, site-directed labeling enables the determination of the membrane localization of the different protein domains as well as of the individual amino acid residues in great detail.

Membrane Assembly of the M13 Major Coat Protein. The λ_{max} plots presented in Figures 4 and 5 are indicative of a protein that is almost entirely embedded in the membrane. This is in accordance with previously observed results (*10*). The minor variations in λ_{max} values of the AEDANS attached to the different positions of the coat protein observed in Figure 5 could be due to small differences in polarity and hydration in the phospholipid headgroup region (*30*). However, the overall λ_{max} profile is remarkably identical for pure DOPC, 80% DOPC/20% DOPG (molar ratio), and 70% DOPE/30% DOPG (molar ratio) membranes. This latter phospholipid composition mimics that of the inner membrane of *E. coli* with respect to the headgroup composition and average hydrophobic thickness (*31*). This result indicates that the embedment of the M13 major coat protein is mainly dominated by hydrophobic interactions. On the basis of the high ratio of ellipticities at 210 and 222 nm observed by circular dichroism (see Figure 8), the overall conformation of the protein in these membranes is mainly α-helical.

The membrane location of the various domains of the coat protein can clearly be deduced from the fitted line in Figure 4. If one starts from the N-terminus of the domain comprising amino acid residues 7−16/17, the fitted line shows a small decrease in λ_{max} values of the AEDANS probe. The λ_{max} value trend line further decreases, indicating that amino acid residues 16/17 to ∼34 of the protein penetrate more deeply into the membrane. From position 34 to 47, the fitted line increases again, almost as an exact mirror of the decreasing section. This indicates that the protein has crossed the membrane center and is now passing through the second leaflet of the bilayer toward the water phase. The mirror property of the fitted lines around position 34 strongly suggests that the protein region from amino acid residue 17 to 47 comprises the transmembrane helical structure, where residues 18 and 46 are located approximately at the membrane−water interface, with position 34 approximately being in the center of the membrane.

Tilted State of the Transmembrane Helical Domain of the Coat Protein. A closer look at the fluctuations of the λ_{max} values around the fitted line in Figure 4 reveals another interesting property of the membrane-spanning protein helix ranging from amino acid residue 17 to 46. This is illustrated in Figure 9, which shows a helical network representation of this protein segment. There is a consistent pattern of amino acid residue positions with relatively high λ_{max} values (denoted with red symbols) being at one side of the helix and the ones with relatively low values (denoted with blue symbols) being at the other side with a crossover around the middle position, which is around position 34. In the case of the first group, the AEDANS label monitors a more polar surrounding. This should be related to the sites of attachment, which are pointing toward the water face. In contrast, probes attached to the residues at the opposite face of the helix should be directed to the hydrophobic membrane interior.

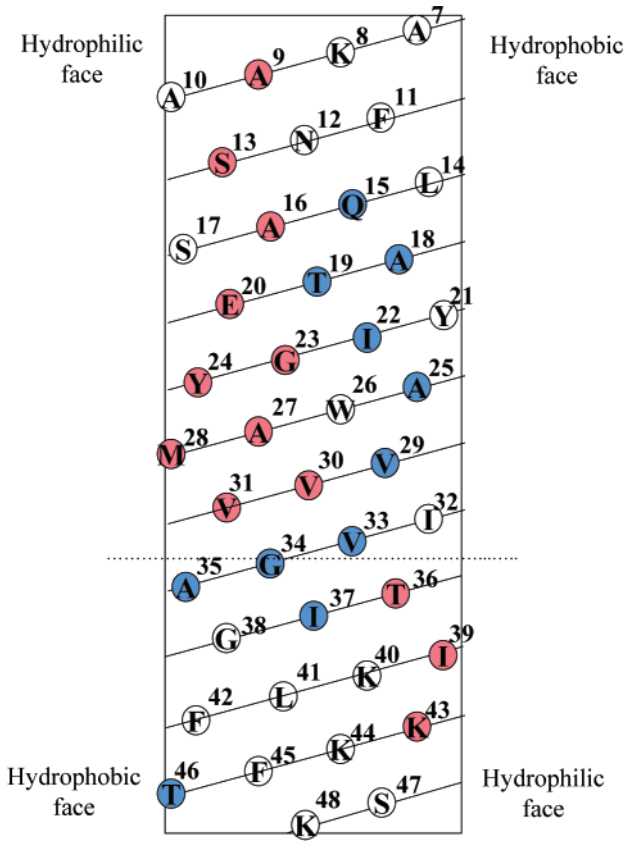

FIGURE 9: Helical network representation of the M13 major coat protein segment from alanine 7 to lysine 48. The amino acids positions that report a relative hydrophilic membrane location (i.e., positions with a relatively high value of λ_{max} with respect to those of their neighboring residues; located at least 1 nm above the curve fit line in Figure 4) are denoted with red symbols. Positions that report a relative hydrophobic membrane location (i.e., positions with a relatively low value of λ_{max} with respect to those of their neighboring residues; located at least 1 nm below the curve fit line in Figure 4) are denoted in blue. The hydrophobic and hydrophilic faces on the helical surface switch at the middle position (shown by the dotted line), which is around position 34. This effect indicates that the helix is tilted with respect to the normal of the bilayer.

Clearly, a hydrophobic and a hydrophilic face can be distinguished on this transmembrane helix. For a helix perpendicular to the bilayer, the two faces of the helix should be indistinguishable. Therefore, this observation indicates that the helix is tilted with respect to the normal of the bilayer. Such a tilted orientation of the transmembrane hydrophobic helix is in agreement with previously reported results (*6*, *11*, *12*). The relative hydrophilic location of labeled mutants L41C and F42C (λ_{max} values of AEDANS are too relatively high in Figure 4) do not well fit into the crossover pattern of a tilted helix. The membrane-anchoring interactions of the C-terminal part of the coat protein are probably affected when these positions are replaced and labeled. This could result in a small outward directed shift of the helical domain, a local conformational change by fraying of the C-terminal end, or an altered tilt angle. In the opposite case, substitutions of polar residues lysine 43 and lysine 44 probably result in λ_{max} values of AEDANS that are too relatively low in Figure 4. These observations are in agreement with the strong membrane anchoring of the C-terminal side of the major coat protein, provided by the two phenylalanines at positions 42 and 45, and the three lysines at positions 40, 43, and 44 (*11*).

The observation of a tilt in the fluorescence data is in agreement with previous work (*29*). It demonstrates that the λ_{max} values of the AEDANS probe attached to the protein are sufficiently sensitive to pick up a minor structural feature, such as a tilt. It also demonstrates that possible disturbing effects of the probes on the tilt and orientation of the protein are small.

Low-Resolution Model of the Membrane-Bound M13 Major Coat Protein. Data obtained in previous studies were interpreted in favor of an L-shaped form of the membrane-bound coat protein, featuring an approximately 90° angle between the amphipathic and transmembrane helix (*6*−*9*). On the basis of the λ_{max} plots in Figures 4 and 5, the N-terminal arm from amino acid residue 7 to 17 is only slightly tilted with respect to the membrane surface and the transmembrane segment from amino acid residue 17 to 46 is tilted with respect to the membrane normal. This is in good agreement with recent findings in the literature (*6*, *10*, *12*, *21*). Therefore, the angle between the amphipathic and transmembrane helix can be much larger than 90°.

It is tempting to interpret our data in a way that shows the major coat protein has at least part of the time an overall curved helical conformation from amino acid residue ~7 to 46. In this view, the curvature can be easily achieved by flexibility in the intrabackbone hydrogen bonds. Therefore, in a membrane, the major coat protein can be seen as a gently curved and tilted, "banana-shaped" molecule, which is anchored in the membrane−water interface at the C-terminal protein part. Via a comparison of this finding with the secondary structure of the protein in Figure 1B, this indicates that in a phospholipid bilayer the so-called hinge region and transmembrane hydrophobic helix actually comprise one continuous helix. This result is shown in Figure 1D. Apparently, the typical two-dimensional feature of the phospholipid bilayer limits the number of possible orientations of these protein segments relative to each other.

Environmental Probing in Response to the Variation of Membrane Thickness. In Figure 6, one can observe that the λ_{max} values of AEDANS decrease when the bilayer thickness is increased. In agreement with a previous study (*10*), these lower λ_{max} values are concomitant with lower quenching efficiencies, and thus lower accessibilities, by the polar quencher acrylamide in thicker membranes (see also Figure 7). Apparently, the extent of membrane penetration of the major coat protein is increased when the hydrophobic thickness of the membrane is enlarged. On the basis of our sample preparations, the M13 major coat protein mutants can be inserted in PC membranes with different hydrophobic thicknesses. However, care must be taken since the response of a protein to the variation of bilayer thickness can be versatile (*32*). When the protein is reconstituted into the thickest membrane (22:1PC), the protein becomes strongly stressed by the hydrophobic mismatch. Most coat protein mutants remain in a transmembrane configuration. However, the delicate interplay of forces for a few mutants, especially those with mutations in the transmembrane domain affecting its overall hydrophobicity, gives rise to a deviating behavior (see Figure 6) that is assigned, at least partly, to a nontransmembrane configuration. A nontransmembrane configuration could also explain the overall loss of helical conformation of the major coat protein when it is reconstituted into thick membranes (Figure 8).

The overall parallel λ_{max} plots of the AEDANS-labeled major coat protein mutants in membranes with different thicknesses (Figure 6) indicate that the relative membrane location of most labeled positions is not changed dramatically. Therefore, apart from a deeper membrane penetration and some flexibility in the N-terminal arm, the overall configuration of the major coat protein is hardly changed with the variation of bilayer thickness. However, as can be seen more clearly in Figure 7, significant effects show up in the hinge region. Most remarkable are the relative constant λ_{max} values of positions 18−24 in the thinnest 14:1PC membrane, and the significant decrease in the λ_{max} values of positions 18 and 22 with an increased bilayer thickness. This relative difference in λ_{max} values coincides roughly with the relative difference in accessibility for the polar quencher acrylamide (Figure 7B). The almost constant λ_{max} values in 14:1PC suggest that positions 18−24 are in an environment with a similar polarity and, thus, comparable membrane location. This can be explained by a stretched (less helical) conformation of this protein segment, oriented parallel to the membrane surface. The observed effect of membrane thickness on the λ_{max} values at positions 18 and 22 in Figure 7 is most obvious when going from the 14:1PC to the 18:1PC system. This illustrates that the hinge region becomes strongly stressed with a hydrophobic thickness smaller than ~23 Å.

The relatively strong decrease in the λ_{max} values at positions 18 and 22 is supported by the concomitant decreased accessibility to the quencher acrylamide (Figure 7), and can be explained by a local conformational change of the hinge segment. Apparently, the initially less structured segment (in the thinnest membrane) changes toward a more helical conformation in thicker membranes (Figure 1C,D) such that backbone positions 18 and 22 point to the membrane interior. This local conformational change is related to internal hydrogen bond formation as a result of a more hydrophobic location of the hinge backbone moieties in the thicker membranes. This relocation results in the promotion of helix conformation by internal hydrogen bonds (*33*). This finding is in agreement with the results of determination of the overall conformation of the protein using CD (Figure 8), where an increase in the amount of helix is observed upon going from the 14:1PC system to the 18:1PC system. A further increase in membrane thickness is expected to enhance the local promotion of helix formation within the hinge segment of the protein (Figure 7), although the overall conformation of the entire protein indicates an overall loss of helical structure (Figure 8). This latter effect is probably due the loss of helical conformation in another protein segment or due to a changed (nontransmembrane) configuration of a part of the protein population.

Response of the M13 Major Coat Protein to Hydrophobic Mismatch. The response of a membrane protein to the variation of bilayer thickness can be versatile; aggregation of the protein, alteration of helix tilt angle, adopting a nontransmembrane configuration, and backbone conformational change can be involved (*32*). Some of these effects can be observed in the case of the M13 major coat protein under hydrophobic mismatch conditions. Previously, the M13 major coat protein was found to be essentially monomeric in mixtures of PC with a varied acyl chain length (*17*). Recently, we presented a change in the tilt angle and orientation of the transmembrane helix of the M13 major coat protein (*29*). Here we show an overall change in penetration depth, the local folding and/or unfolding of a flexible protein segment, and the adoption of a nontransmembrane configuration to be involved as well. In addition, the "elastic" lipid bilayer can adapt to the protein. It should be noted that all these determinants could contribute to some extent to a stable membrane-bound state of the M13 major coat protein.

Biological Implications. Conformational flexibility of the hinge region allows the major coat protein to be nicely accommodated in membranes with a varying hydrophobic thickness. When all results are taken into account, an intermediate and adjustable structure of the coat protein can be proposed. On average, this structure will shuttle between an extreme L-shaped form as reported previously (*6*−*9*) and a slightly bent I-shaped form [as present in the phage particle; see Figure 1E (*13*)]. Such an "average" conformation would look like a banana-shaped form, which is strongly anchored in the membrane at the C-terminus (*11*).

A structural and dynamical adaptation of the major coat protein seems to provide the most likely reversible mechanism for responding to environmental changes during the bacteriophage disassembly and assembly process (*1*). A small local change in hydrogen bonding can result in a large change in protein structure and topology. In this view, there actually is only a small conformational difference between the state of the coat protein when it is part of the phage particle and the state of the coat protein when it is embedded in the *E. coli* inner membrane.

ACKNOWLEDGMENT

We are very grateful to Dr. David Stopar (Biotechnical Faculty, University of Ljubljana, Ljubljana, Slovenia) for the help with the CD measurements and the helpful and stimulating discussions.

REFERENCES

1. Marvin, D. A. (1998) Filamentous phage structure, infection and assembly, *Curr. Opin. Struct. Biol. 8*, 150−158.
2. Stopar, D., Spruijt, R. B., Wolfs, C. J. A. M., and Hemminga, M. A. (2003) Protein−Lipid interactions of bacteriophage M13 major coat protein, *Biochim. Biophys. Acta 1611*, 5−15.
3. Lee, A. G. (2003) Lipid−protein interactions in biological membranes: a structural perspective, *Biochim. Biophys. Acta 1612*, 1−40.
4. Almeida, F. C. L., and Opella, S. J. (1997) Fd coat protein structure in membrane environments: Structural dynamics of the loop between the hydrophobic trans-membrane helix and the amphipathic in-plane helix, *J. Mol. Biol. 270*, 481−495.
5. Papavoine, C. H. M., Christiaans, B. E. C., Folmer, R. H. A., Konings, R. N. H., and Hilbers, C. W. (1998) Solution structure of the M13 major coat protein in detergent micelles: A basis for a model of phage assembly involving specific residues, *J. Mol. Biol. 282*, 401−419.
6. Marassi, F. M., and Opella, S. J. (2003) Simultaneous assignment and structure determination of a membrane protein from NMR orientational restraints, *Protein Sci. 12*, 403−411.
7. McDonnell, P. A., Shon, K., Kim, Y., and Opella, S. J. (1993) Fd coat protein structure in membrane environments, *J. Mol. Biol. 233*, 447−463.
8. Marassi, F. M., Ramamoorthy, A., and Opella, S. J. (1997) Complete resolution of the solid state NMR spectrum of a uniformly ^{15}N labeled membrane protein in phospholipid bilayers, *Proc. Natl. Acad. Sci. U.S.A. 94*, 8551−8556.
9. Wolkers, W. F., Spruijt, R. B., Kaan, A., Konings, R. N. H., and Hemminga, M. A. (1997) Conventional and saturation transfer

EPR of spin labeled mutant bacteriophage M13 coat protein in phospholipid bilayers, *Biochim. Biophys. Acta 1327*, 5−16.
10. Spruijt, R. B., Meijer, A. B., Wolfs, C. J. A. M., and Hemminga, M. A. (2000) Localization and rearrangement modulation of the N-terminal arm of the membrane-bound major coat protein of bacteriophage M13, *Biochim. Biophys. Acta 1509*, 311−323.
11. Meijer, A. B., Spruijt, R. B., Wolfs, C. J. A. M., and Hemminga, M. A. (2001) Membrane-anchoring interactions of M13 major coat protein, *Biochemistry 40*, 8815−8820.
12. Glaubitz, C., Grobner, G., and Watts, A. (2000) Structural and orientational information of the membrane embedded M13 coat protein by C-13-MAS NMR spectroscopy, *Biochim. Biophys. Acta 1463*, 151−161.
13. Marvin, D. A., Hale, R. D., Nave, C., and Citterich, M. H. (1994) Molecular models and structural comparisons of native and mutant class-I filamentous bacteriophages Ff (fd, f1, M13), If1 and Ike, *J. Mol. Biol. 235*, 260−286.
14. Spruijt, R. B., and Hemminga, M. A. (1991) The in situ aggregational and conformational state of the major coat protein of bacteriophage M13 in phospholipid bilayers mimicking the inner membrane of host *Escherichia coli*, *Biochemistry 30*, 11147−11154.
15. Li, Z. M., Glibowicka, M., Joensson, C., and Deber, C. M. (1993) Conformational states of mutant M13 coat proteins are regulated by transmembrane residues, *J. Biol. Chem. 268*, 4584−4587.
16. Haigh, N. G., and Webster, R. E. (1998) The major coat protein of filamentous bacteriophage f1 specifically pairs in the bacterial cytoplasmic membrane, *J. Mol. Biol. 279*, 19−29.
17. Fernandes, F., Loura, L. M. S., Prieto, M., Koehorst, R. B. M., Spruijt, R. B., and Hemminga, M. A. (2003) Dependence of M13 major coat protein oligomerization and lateral segregation on bilayer composition, *Biophys. J. 85*, 2430−2441.
18. Torres, J., Stevens, T. J., and Samso, M. (2003) Membrane proteins: the "Wild West" of structural biology, *Trends Biochem. Sci. 28*, 137−144.
19. Spruijt, R. B., Wolfs, C. J. A. M., Verver, J. W. G., and Hemminga, M. A. (1996) Accessibility and environment probing using cysteine residues introduced along the putative transmembrane domain of the major coat protein of bacteriophage M13, *Biochemistry 35*, 10383−10391.
20. Stopar, D., Spruijt, R. B., Wolfs, C. J. A. M., and Hemminga, M. A. (1996) Local dynamics of the M13 major coat protein in different membrane-mimicking systems, *Biochemistry 35*, 15467−15473.
21. Meijer, A. B., Spruijt, R. B., Wolfs, C. J. A. M., and Hemminga, M. A. (2001) Configurations of the N-terminal amphipathic domain of the membrane-bound M13 major coat protein, *Biochemistry 40*, 5081−5086.
22. Hudson, E. N., and Weber, G. (1973) Synthesis and Characterization of Two Fluorescent Sulfhydryl Reagents, *Biochemistry 12*, 4154−4161.
23. Schägger, H., and Von Jagow, G. (1987) Tricine-sodium dodecyl sulfate-polyacrylamide gel electrophoresis for the separation of proteins in the range from 1 to 100 kDa, *Anal. Biochem. 166*, 368−379.
24. Spruijt, R. B., Wolfs, C. J. A. M., and Hemminga, M. A. (1989) Aggregation-related conformational change of the membrane-associated coat protein of bacteriophage M13, *Biochemistry 28*, 9158−9165.
25. De Planque, M. R. R., Goormagtigh, E., Greathouse, D. V., Koeppe, R. E., II, De Kruijtzer, J. A. W., Liskamp, R. M. J., De Kruijff, B., and Killian, J. A. (2001) Sensitivity of single membrane-spanning α-helical peptides to hydrophobic mismatch with a lipid bilayer: effects on backbone structure, orientation, and extent of membrane incorporation, *Biochemistry 40*, 5000−5010.
26. Ridder, A., van de Hoef, W., Stam, J., Kuhn, A., de Kruijff, B., and Killian, J. A. (2002) Importance of hydrophobic matching for spontaneous insertion of a single-spanning membrane protein, *Biochemistry 41*, 4946−4952.
27. Lehrer, S. S., and Leavis, P. C. (1978) Solute quenching of protein fluorescence, *Methods Enzymol. 49*, 222−236.
28. Sanders, J. C., Haris, P. I., Chapman, D., Otto, C., and Hemminga, M. A. (1993) Secondary structure of M13 coat protein in phospholipids studied by circular dichroism, Raman, and Fourier transform infrared spectroscopy, *Biochemistry 32*, 12446−12453.
29. Koehorst, R. B. M., Spruijt, R. B., Vergeldt, F. J., and Hemminga, M. A. (2004) Lipid bilayer topology of the transmembrane α-helix of M13 major coat protein and bilayer polarity profile by site-directed fluorescence spectroscopy, *Biophys. J. 87*, 1445−1455.
30. Meijer, A. B., Spruijt, R. B., Wolfs, C. J. A. M., and Hemminga, M. A. (2000) Membrane assembly of the bacteriophage Pf3 major coat protein, *Biochemistry 39*, 6157−6163.
31. Burnell, E., Van Alphen, L., Verkleij, A., and De Kruijff, B. (1980) Phosphorus-31 nuclear magnetic resonance and freeze-fracture electron microscopy studies on *Escherichia coli*. I. Cytoplasmic membrane and total phospholipids, *Biochim. Biophys. Acta 597*, 492−501.
32. Killian, J. A. (1998) Hydrophobic mismatch between proteins and lipids in membranes, *Biochim. Biophys. Acta 1376*, 401−416.
33. Hemminga, M. A., Sanders, J. C., and Spruijt, R. B. (1992) Spectroscopy of lipid protein interactions; Structural aspects of two different forms of the coat protein of bacteriophage M13 incorporated in model membranes, *Prog. Lipid Res. 31*, 301−333.

BI048437X